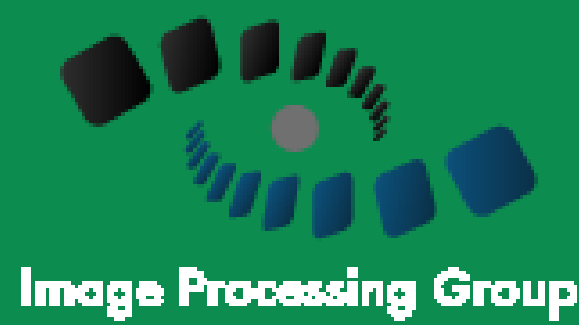


Motion Inpainting by an Image-Based Geodesic AMLE Method



M. Oliver, L. Raad (lara.raad@upf.edu), G. Haro, C. Ballester
Universitat Pompeu Fabra (Barcelona, Spain)



1 Introduction

- An **optical flow inpainting** method is proposed using a metric-based anisotropic diffusion method.
- From the video pixel values a Riemannian metric is defined on each frame, guiding the interpolation.
- The missing optical flow is recovered by solving the **AMLE PDE** on the Riemannian manifold.
- The aim is to recover the optical flow while correctly **handling the motion discontinuities** of the objects.

3 Proposed model

Let us consider a video $I(\mathbf{x}, t)$ defined on $\Omega \subset \mathbb{R}^2 \times \{1, \dots, T\}$. Its optical flow $\mathbf{v}(\mathbf{x}, t) = (v_1, v_2)$ is unknown on a region $\Omega_0(t) \subset \Omega$ with boundary $\partial\Omega_0(t)$. At each time t , the domain Ω is endowed with a metric $g(t)$ and the corresponding Riemannian manifold is denoted by $\mathcal{M}(t) = (\Omega, g(t))$. The optical flow is inpainted with $\mathbf{u} = (u_1, u_2)$ such that each u_i is a solution of the geodesic **Absolutely Minimizing Lipschitz Extension (AMLE)**, defined by the following PDE and coupled with Neumann boundary conditions:

$$\Delta_{\infty, g} u_i = 0 \quad \text{in } \Omega_0(t) \quad \text{s.t.} \quad u_i|_{\partial\Omega_0(t)} = v_i, \quad i = 1, 2$$

where $\Delta_{\infty, g} u_i := D_{\mathcal{M}}^2 u_i \left(\frac{\nabla_{\mathcal{M}} u_i}{|\nabla_{\mathcal{M}} u_i|}, \frac{\nabla_{\mathcal{M}} u_i}{|\nabla_{\mathcal{M}} u_i|} \right)$ is the infinity Laplacian and $\nabla_{\mathcal{M}} u_i$ and $D_{\mathcal{M}}^2 u_i$ are the gradient and the Hessian on the manifold $\mathcal{M}(t)$.

3.1 The geodesic AMLE on a finite graph

1. Positive and negative eikonal operators [2]

$$\|\nabla u(\mathbf{x})\|_{\mathcal{M}}^+ = \max_{\mathbf{y} \in \mathcal{N}(\mathbf{x})} \frac{u(\mathbf{y}) - u(\mathbf{x})}{d^g(\mathbf{x}, \mathbf{y})}, \quad \|\nabla u(\mathbf{x})\|_{\mathcal{M}}^- = \min_{\mathbf{z} \in \mathcal{N}(\mathbf{x})} \frac{u(\mathbf{z}) - u(\mathbf{x})}{d^g(\mathbf{x}, \mathbf{z})}$$

2. The discrete infinity Laplacian corresponds to

$$\Delta_{\infty, g} u(\mathbf{x}) = \frac{\|\nabla u(\mathbf{x})\|_{\mathcal{M}}^+ + \|\nabla u(\mathbf{x})\|_{\mathcal{M}}^-}{2}$$

3. We use the following iterative discrete scheme

$$u^{k+1}(\mathbf{x}) = \frac{d^g(\mathbf{x}, \mathbf{z})u^k(\mathbf{z}) + d^g(\mathbf{x}, \mathbf{y})u^k(\mathbf{y})}{d^g(\mathbf{x}, \mathbf{z}) + d^g(\mathbf{x}, \mathbf{y})}$$

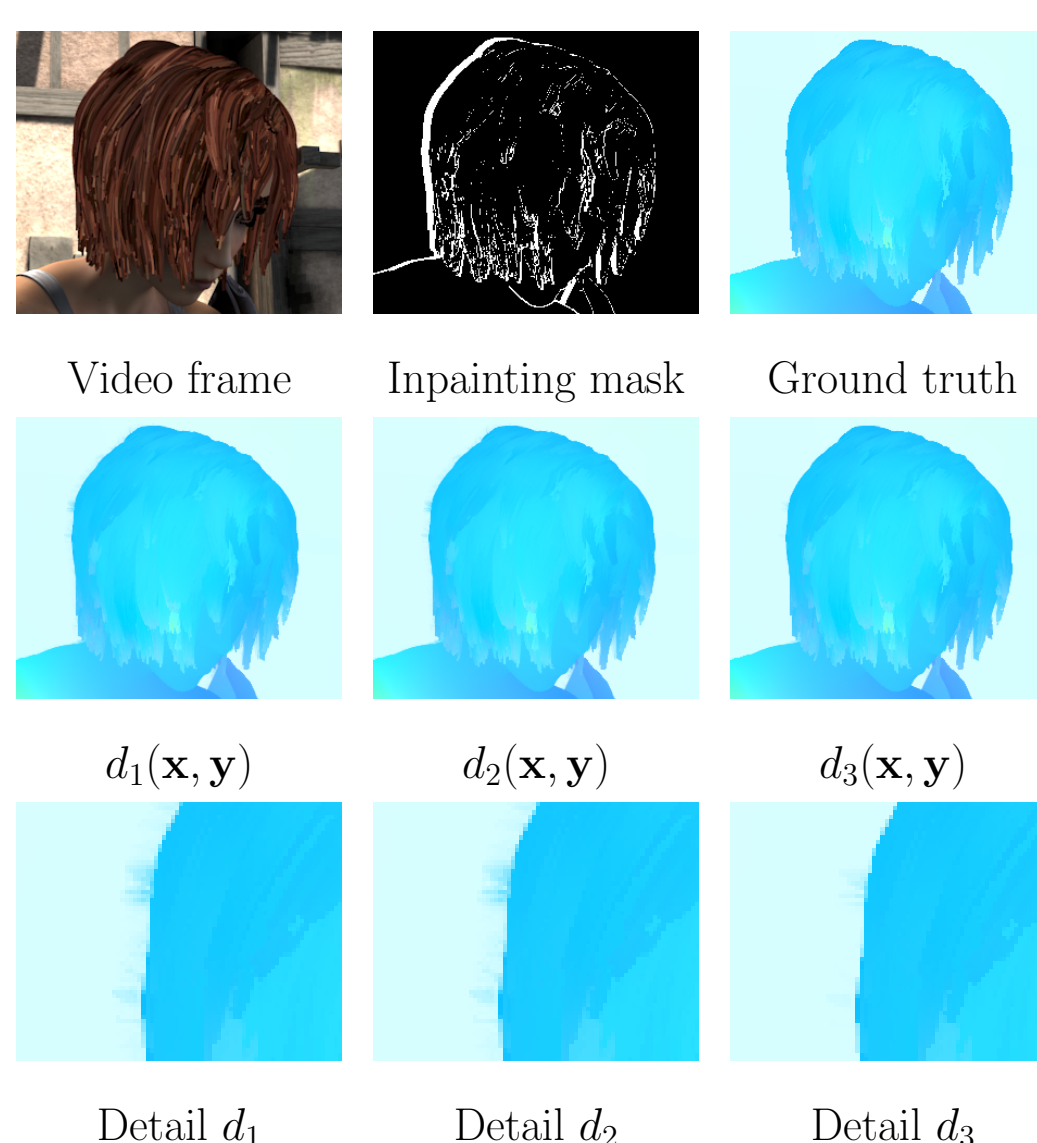
3.2 Distance d^g

Given any two points \mathbf{x} and \mathbf{y} the geodesic distance is:

$$d^g(\mathbf{x}, \mathbf{y}) = \inf \left\{ \sum_{i=0}^{m-1} d(\gamma(i), \gamma(i+1)) : \gamma \text{ is a curve joining } \mathbf{x} \text{ and } \mathbf{y} \right\}$$

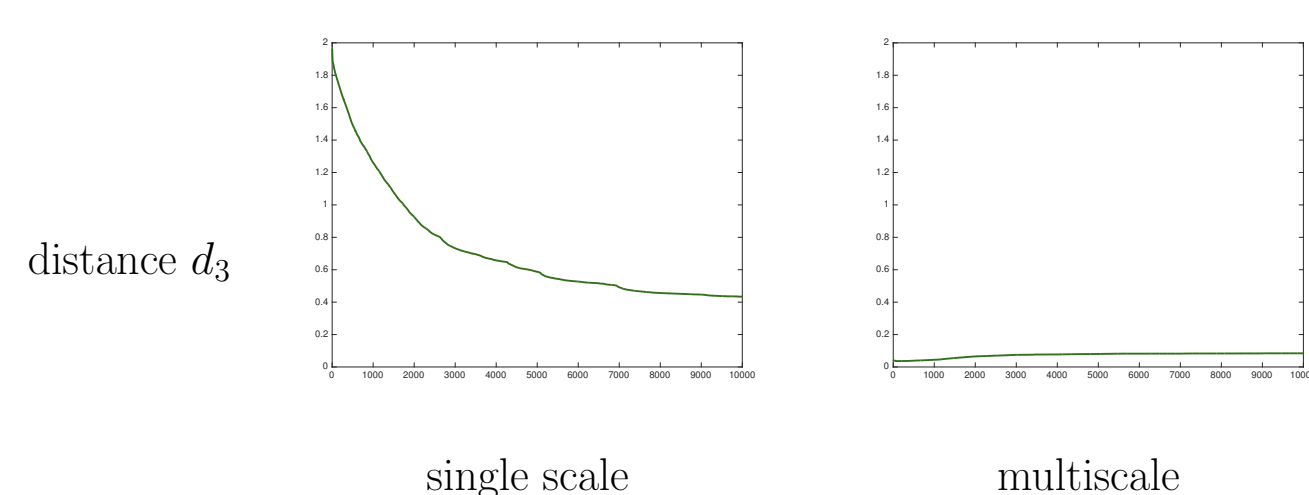
For any pair of points \mathbf{x}, \mathbf{y} we approximate $d^g(\mathbf{x}, \mathbf{y})$ by $d(\mathbf{x}, \mathbf{y})$ defined by:

- $d_1(\mathbf{x}, \mathbf{y}) = \sqrt{(1-\lambda)\|I(\mathbf{x}, t) - I(\mathbf{y}, t)\|^2 + \lambda\|\mathbf{x} - \mathbf{y}\|^2}$
- $d_2(\mathbf{x}, \mathbf{y}) = (1-\lambda)\|I(\mathbf{x}, t) - I(\mathbf{y}, t)\| + \lambda\|\mathbf{x} - \mathbf{y}\|$
- $d_3(\mathbf{x}, \mathbf{y}) = (1-\lambda)\|I(\mathbf{x}, t) - I(\mathbf{y}, t)\|^2 + \lambda\|\mathbf{x} - \mathbf{y}\|^2$



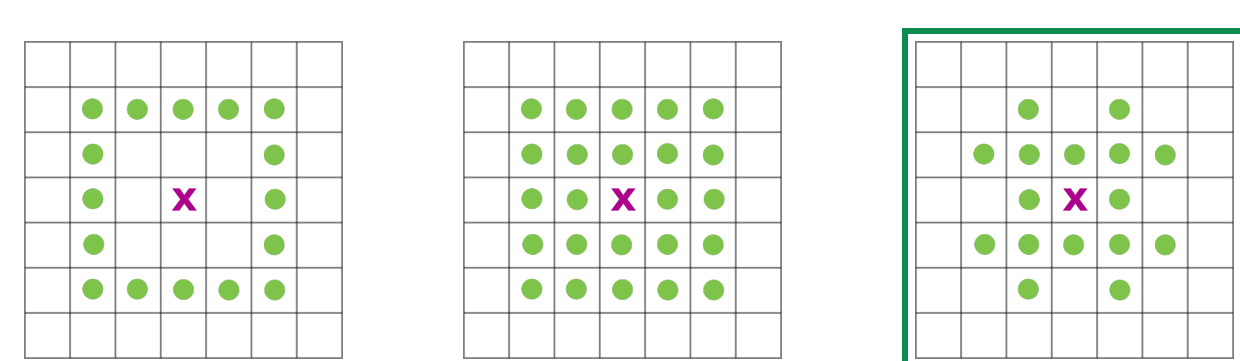
3.3 Multiscale approach

A multiscale pyramid leads to a faster convergence. At the coarsest level, the unknowns are initialized to zero; the other scales are initialized by upsampling the solution of the previous scale.



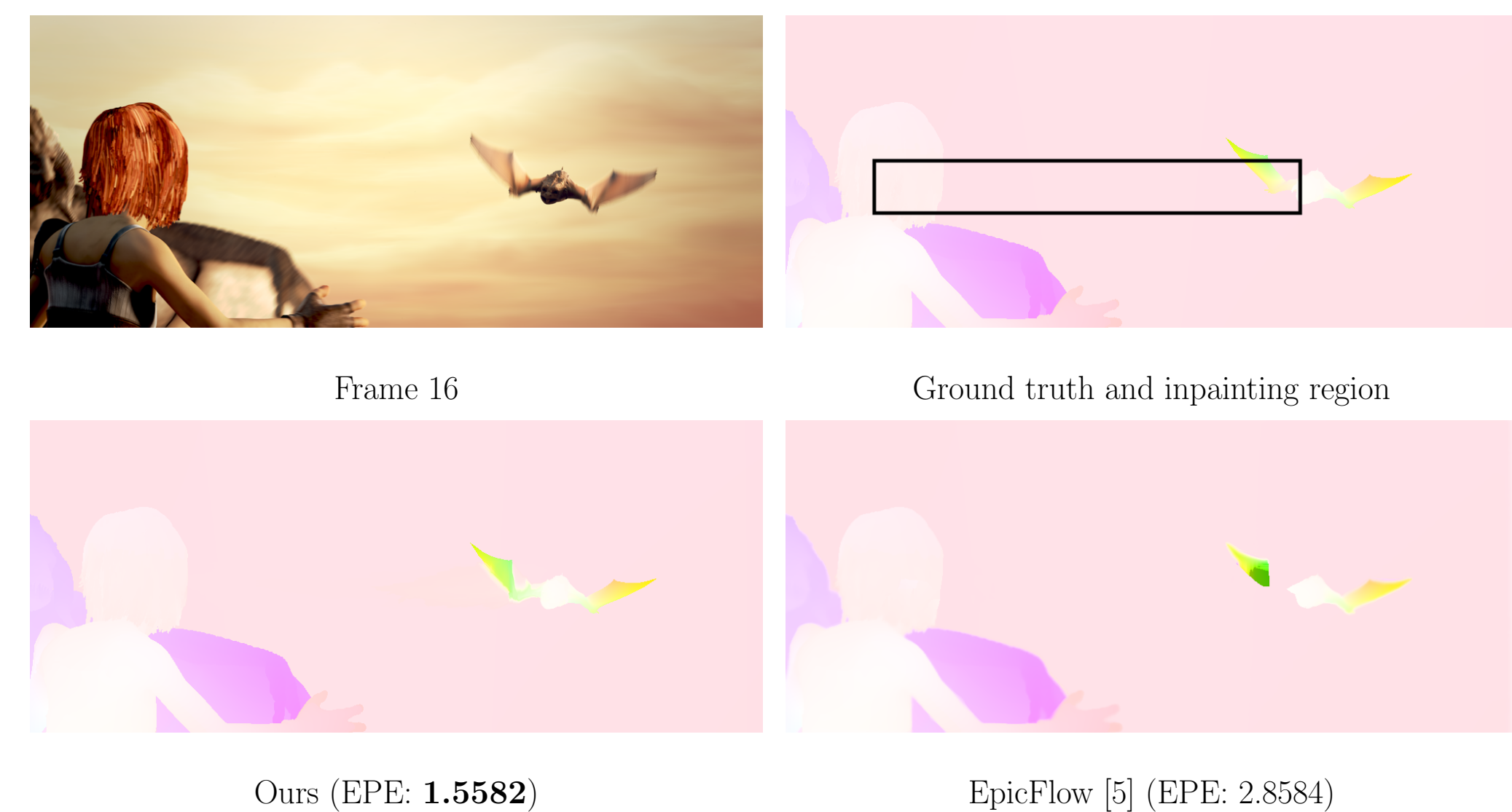
3.4 Neighbourhood type

The solution of the numerical scheme converges to the solution of the continuous AMLE PDE when the spatial and directional resolution tend to zero [3]. Three neighbourhoods were evaluated:



The neighbourhood on the right hand gives the best compromise between spatial and directional resolution and number of samples.

2 An inpainting example

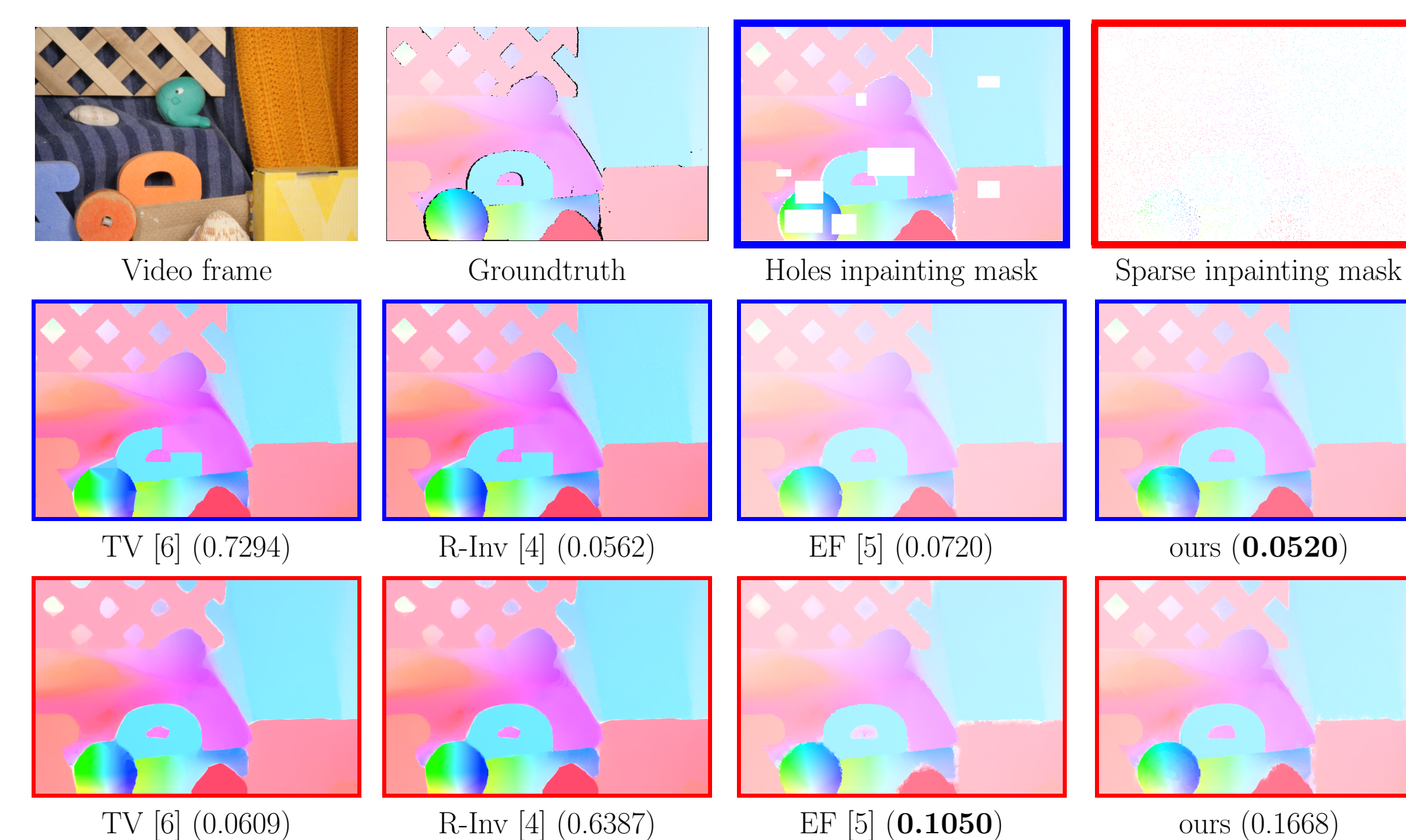


4 Results

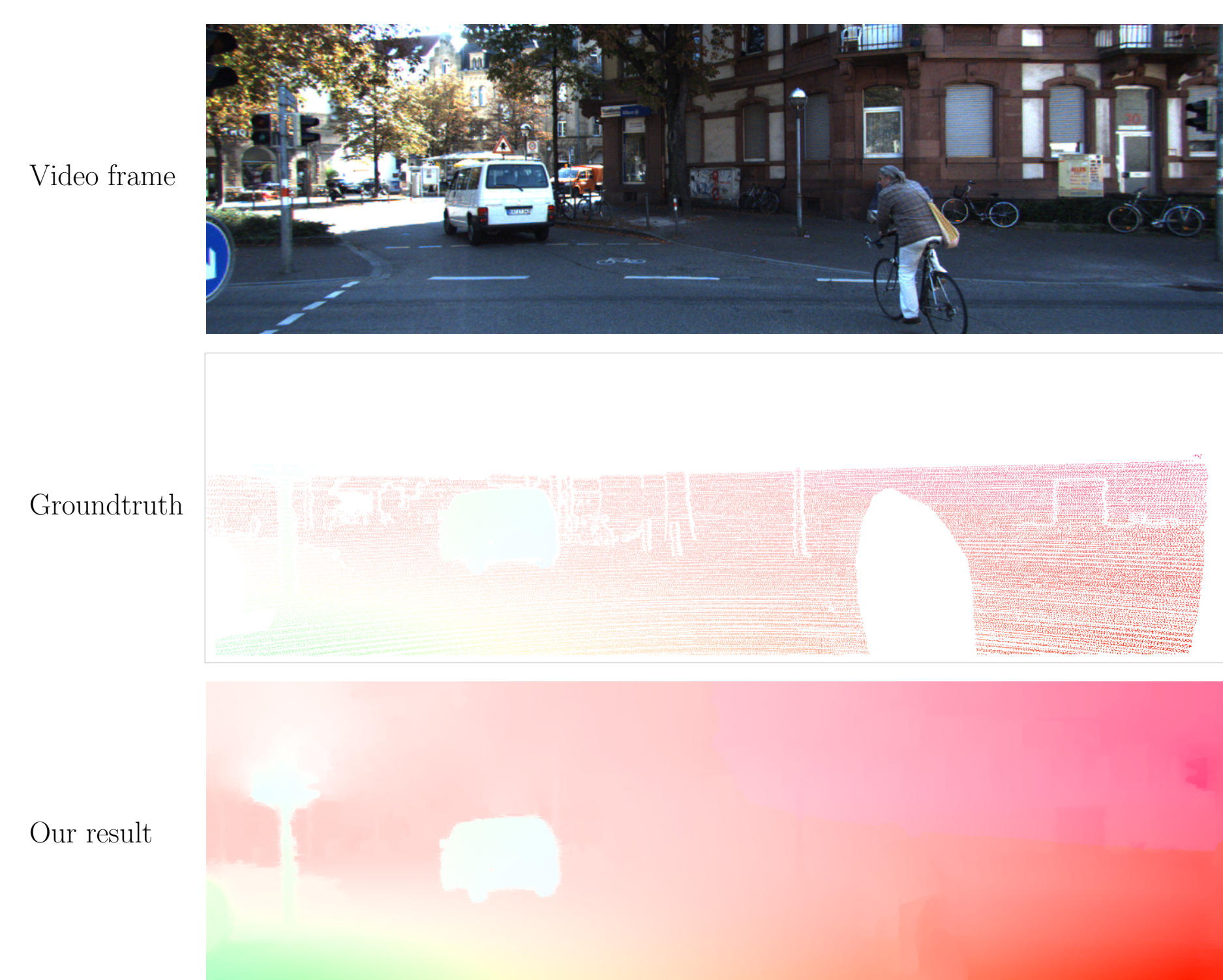
End-Point-Error: comparative tables

	SINTEL		MIDDLEBURY	
	Ours	EF [5]	Ours	EF [5]
occlusions	5.4198	6.8797	-	-
sparse 1%	0.7061	1.8532	0.1979	0.3105
sparse 5%	0.4340	1.4199	0.1053	0.2426
sparse 30%	0.2241	1.1212	0.0567	0.1801
sparse dm	4.4404	4.1507	0.9216	0.8112
sparse dm-gt	2.1360	2.3802	0.2049	0.2789
hole	1.7208	1.9587	-	-

Comparative visual results on MIDDLEBURY data



Inpainting of large holes on data from KITTI dataset



5 Conclusions

The proposed method produces good results for:

- Optical flow densification
- Motion completion in large holes
- Motion completion in occluded areas

6 Future work

- Exploration of alternative metrics
- Extension to a vectorial AMLE model
- Extension to a joint video and optical flow inpainting

7 References

- [1] G. Aronsson (Ark. Mat., 1967)
- [2] J. J. Manfredi and A. M. Oberman (Dif. Int. Eq., 2015)
- [3] A. M. Oberman (Math. Comput., 2005)
- [4] R. P. Palomares et al. (ACCV, 2014)
- [5] J. Revaud et al. (IJCV, 2016)
- [6] L. I. Rudin (Physica D, 1992)